

1 **Altered innate defenses in the neonatal gastrointestinal tract in response to**
2 **colonization by neuropathogenic *Escherichia coli***

3
4 George M.H. Birchenough,^{a†} Malin E.V. Johansson,^b Richard A. Stabler,^c Fatma
5 Dalgakiran,^a Gunnar C. Hansson,^b Brendan W. Wren,^c J. Paul Luzio,^d and Peter W.
6 Taylor^{a#}

7
8 ^aUniversity College London School of Pharmacy, London, WC1N 1AX, United Kingdom

9 ^b Mucin Biology Group, University of Gothenburg, SE-405 30 Gothenburg, Sweden

10 ^cLondon School of Hygiene and Tropical Medicine, London WC1E 7HT, United
11 Kingdom

12 ^dCambridge Institute for Medical Research, University of Cambridge, Cambridge CB2
13 0XY, United Kingdom

14
15 [#]Correspondence footnote: Peter Taylor, School of Pharmacy, University College
16 London, 29-39 Brunswick Square, London WC1N 1AX, UK; tel +44 20 7753 5867; fax
17 +44 20 7753 5942; peter.taylor@ucl.ac.uk

18
19 Running title: Colonization of neuropathogenic *E. coli*

20
21
22 [†]Current address: Mucin Biology Group, University of Gothenburg, SE-405 30
23 Gothenburg, Sweden

24 **ABSTRACT**

25 Two-day-old (P2), but not nine-day-old (P9), rat pups are susceptible to systemic
26 infection following gastrointestinal colonization by *Escherichia coli* K1. Age dependency
27 reflects the capacity of colonizing K1 to translocate from gastrointestinal (GI) tract to
28 blood. A complex GI microbiota developed by P2, showed little variation over P2-P9 and
29 did not prevent stable K1 colonization. Substantial developmental expression was
30 observed over P2-P9, including up-regulation of genes encoding components of the small
31 intestinal (α -defensins Defa24 and Defa-rs1) and colonic (trefoil factor Tff2) mucus
32 barrier. K1 colonization modulated expression of these peptides: developmental
33 expression of Tff2 was dysregulated in P2 tissues and was accompanied by a decrease in
34 mucin Muc2. Conversely, α -defensin genes were up-regulated in P9 tissues. We propose
35 that incomplete development of the mucus barrier during early neonatal life and the
36 capacity of colonizing K1 to interfere with mucus barrier maturation provide
37 opportunities for neuropathogen translocation into the bloodstream.

38

39

40

41

42

43

44

45

46

47 **INTRODUCTION**

48 The newborn infant is particularly vulnerable to systemic bacterial infection during the
49 first four weeks of life and mortality and morbidity associated with neonatal bacterial
50 meningitis (NBM) and accompanying sepsis remain significant despite advances in
51 antibacterial chemotherapy and supportive care (1, 2). In the developed world,
52 *Escherichia coli* and Group B streptococci are responsible for the majority of cases of
53 NBM and bacteria isolated from the cerebrospinal fluid of infected neonates invariably
54 elaborate a protective polysaccharide capsule. Of neuroinvasive *E. coli* isolates, 80-85%
55 express the K1 capsule (3, 4), a homopolymer of α -2,8-linked polysialic acid (polySia)
56 that mimics the molecular structure of the polySia modulator of neuronal plasticity in
57 mammalian hosts (5) and enables these strains to evade detection by a neonatal innate
58 immune system undergoing a process of age-dependent maturation (6).

59 Risk factors for NBM include obstetric and perinatal complications, premature birth
60 and low birth weight, particularly in low socioeconomic groups (7), but predisposition to
61 infection is critically dependent on vertical transmission of the causative agent from the
62 mother to infant at, or soon after, birth (8). Although many aspects of the pathogenesis of
63 *E. coli* K1 in NBM are unclear, maternally-derived *E. coli* K1 bacteria are known to
64 colonize the neonatal gastrointestinal (GI) tract (8, 9, 10), which is sterile at birth but
65 rapidly acquires a complex microbiota that eventually converges toward a profile
66 characteristic of the adult GI tract (11). *E. coli* K1 bacteria then translocate from the
67 lumen of the small intestine or colon into the systemic circulation before entering the
68 CNS across the blood-brain barrier at the cerebral microvascular endothelium of the

69 arachnoid membrane (12) or the blood-cerebrospinal fluid (CSF) barrier at the choroid
70 plexus epithelium (13).

71 Many of the temporal and spatial aspects of NBM can be reproduced in a rodent
72 model of *E. coli* K1 infection initially developed by Glode et al. (14) and subsequently
73 refined by others (15, 16). Thus, oral (15, 16, 17) or intragastric (14, 18) administration of
74 *E. coli* K1 results in stable and persistent GI colonization of adults and neonates. *E. coli*
75 K1-colonized neonatal rat pups, but not adult animals, subsequently develop lethal
76 systemic infection, with *E. coli* K1 present in the blood circulation and brain tissue (15,
77 19, 20). Persistence of bacteria in the blood is dependent on the continued expression of
78 the polySia capsule, as evidenced by the inability of capsule defective mutants to cause
79 systemic infection (21) and by the capacity of intraperitoneally delivered capsule-
80 selective depolymerase to abrogate infection (16). Bacteria enter the CSF compartment of
81 infected rat pups predominantly at the choroid plexus and penetrate superficial brain
82 tissue (19), where they induce inflammation *via* proinflammatory cytokine-induced
83 pathways involving IL-1 β , IL-6 and TNF- α (20).

84 The experimental rodent model of infection has yielded fresh insights into the transit
85 of the *E. coli* K1 neuropathogen from the blood circulation into the CNS; in particular,
86 the age-dependency of experimental NBM in rodents is striking, with clear evidence of
87 systemic infection at two days of age. We now employ this model to shed light on the
88 mechanism of bacterial translocation from the GI tract to the blood compartment. As it is
89 unlikely that conventional prophylactic measures such as vaccination can be readily
90 implemented to prevent infection in the at-risk neonatal cohort - the poor immunogenicity
91 of polySia, the relative unresponsiveness of the neonatal immune system, lack of IgA-

92 mediated protection of mucosal surfaces and the age profile of the target patient
93 population mitigate against the successful development of vaccination as a preventative
94 strategy for the control of *E. coli* NBM (22, 23) – a more detailed understanding of the
95 early stages of NBM will underpin alternative approaches to the prevention of *E. coli* K1
96 systemic neonatal infection, such as bacteriophage-mediated selective elimination of the
97 *E. coli* K1 bacterial cohort from maternal or neonatal reservoirs, and forms the basis of
98 the study reported here.

99 The preterm rodent GI tract is sterile but becomes colonized immediately after birth
100 (24). Little is known of the dynamics of colonization of the rat GI tract by maternally-
101 derived microbes but any lag in the development of a mature microbiota may allow
102 colonizing *E. coli* K1 to achieve sufficient density in the colon or small intestine to
103 permit entry into the blood circulation during the first few days of life. K1 bacteria transit
104 to the blood from the GI tract *via* the mesenteric lymph nodes and there is compelling
105 evidence that they do so with a very low frequency (15). In the study reported here, we
106 found no evidence that the development of a mature microbiota in neonatal rat pups
107 influenced the size or location within the GI tract of the colonizing *E. coli* K1 population
108 and is unlikely to be responsible for the strong age-dependency of experimental NBM in
109 rodents. There were, however, differences in the appearance of the GI tract between
110 susceptible and non-susceptible animals; tissues of younger, susceptible pups contained
111 fewer goblet cells and the intestinal mucus layer was less developed in comparison to
112 older, resistant animals. We also identified major differences in the capacity of
113 susceptible and non-susceptible neonatal pups to respond to GI tract colonization by *E.*
114 *coli* K1, potentially enabling a closer association of *E. coli* K1 with the epithelial surface

115 in susceptible compared to non-susceptible pups. Further, susceptible rat pups, in contrast
116 to non-susceptible animals, were unable to respond to *E. coli* K1 colonization by
117 increasing the concentrations of the defensin peptides Defa-rs1 and Defa24 in the lumen
118 of the small intestine. These changes were not evident following GI tract colonization by
119 non-pathogenic *E. coli* K12. We propose a model based on these observations to account
120 for the strong age-dependency of *E. coli* K1 NBM.

121

122 **MATERIALS AND METHODS**

123 **Bacterial strains and bacterial colonization of neonatal rat pups.** *E. coli* O18:K1
124 strain A192PP was derived from *E. coli* A192, an isolate from a patient with septicemia
125 (25), by serial passage through neonatal rat pups as described previously (16, 19); the
126 passaged strain was significantly more virulent for rat pups than *E. coli* A192 (17). *E. coli*
127 K12 was obtained from the Coli Genetic Stock Center, Yale University as CGSC5073
128 (K12 wildtype). Wistar rat litters (9-14 individuals), obtained from Harlan UK, were
129 retained in a single cage with their natural mothers after birth. For GI tract colonization,
130 all members of a litter were fed 20 µl of mid-exponential phase Mueller-Hinton (MH)
131 broth culture of *E. coli* K1 ($2-6 \times 10^6$ CFU, warmed to 37°C) from an Eppendorf
132 micropipette. Colonization was determined by MacConkey agar culture of perianal swabs
133 as described earlier (16). Bacteremia was detected by culture on MacConkey agar of
134 daily blood samples taken from superficial veins in the footpad. Animal experiments
135 were approved by the Ethical Committee of UCL School of Pharmacy and the UK Home
136 Office (HO) and were conducted under HO Project Licence PPL 80/2243.

137

138 **Processing of animal material.** Stools were collected from adult animals and neonates
139 were killed by decapitation; *post mortem* the neonatal GI tract, from stomach to colon,
140 was excised aseptically. For *E. coli* K1 enumeration and DNA extraction, samples were
141 transferred to 2 ml ice-cold PBS and homogenized. For enumeration, the homogenate
142 was serially diluted in PBS and plated onto MacConkey agar. Coliform colonies were re-
143 streaked and assayed for sensitivity to the K1-specific lytic phage K1E (26). DNA was
144 extracted from homogenates using the QIAamp Stool DNA Mini Kit (Qiagen). For RNA
145 extraction, tissues were transferred to RNAlater (Ambion) and stored overnight at 4°C.
146 RNA was then extracted using the RNeasy Midi Kit (Qiagen). Nucleic acid extractions
147 were quantified and assessed for purity using a Nanodrop 1000 (Thermo Scientific) and
148 native DNA/RNA agarose gel electrophoresis. For protein extraction, tissues were
149 homogenized in 2 ml tissue lysis buffer containing 1% v/v NP-40, 1% v/v Tween-20 and
150 Tris-EDTA (10mM Tris-HCl, 1mM EDTA, pH 7.4) in PBS supplemented with 1 x
151 Complete Mini EDTA-free protease inhibitor cocktail (Roche). Protein extracts were
152 quantified using Bio-Rad Protein Assay reagent in cuvette format. All homogenizations
153 were performed on ice using an Ultra-Turrax T-10 homogenizer (IKA Werke); extracts
154 were stored at -80°C prior to analysis.

155

156 **GI microbiota profiles**

157 Analysis of the composition of complex microbial communities has been facilitated by an
158 expanding database of small subunit rRNA gene (SSU rDNA) sequences. Palmer et al.
159 (11, 27) designed a microarray-based platform incorporating probes which target the
160 more variable SSU rDNA regions; the customized microarray (Agilent Technologies),

161 used in the current study, consisted of 10,266 unique oligonucleotide sequences covering
162 1,590 bacterial and 39 archeal species as well as 649 higher order taxonomic groups
163 which together ensure broad coverage of known SSU rDNA sequences within the
164 prokaryotic multiple sequence (prokMSA) database ([http://greengenes.lbl.gov/cgi-](http://greengenes.lbl.gov/cgi-bin/nph-index.cgi)
165 [bin/nph-index.cgi](http://greengenes.lbl.gov/cgi-bin/nph-index.cgi)). The platform can be used to quantify different SSU rDNA
166 populations from mixed samples using standard microarray technology. DNA was
167 extracted from three stool samples for each adult and three GI tissue samples per litter for
168 each neonatal age group examined using the QIAamp Stool DNA mini kit. SSU rDNA
169 was amplified from 1 µg extracted DNA using the GoTaq Green PCR kit (Promega) and
170 the broad-range bacteria-specific primers Bact-8F and T7-1391R described by Palmer et
171 al. (11). Amplified DNA was quantified using a Nanodrop 1000 and the products
172 confirmed by agarose gel electrophoresis. A reference pool was constructed from an
173 equimolar mixture of all samples for use as a template for *in vitro* transcription.
174 Reference pool amplicons were labeled with Cy3 and test samples comprising amplified
175 DNA from animals in individual age groups with Cy5 using the gDNA labeling kit plus
176 (Agilent Technologies); combined Cy3/5 labeled samples were purified using MinElute
177 columns (Qiagen). For hybridization, 4.5 µl blocking agent and 22.5 µl hybridisation
178 buffer from Hyb kit (Agilent Technologies) were added to 18 µl of eluted DNA. After 3
179 min at 95°C and 30 min at 37°C, the 45 µl sample was loaded into a hybridization
180 chamber (Agilent Technologies) and the arrays hybridized at 65°C in a rotating oven for
181 24 h. Slides were washed in Oligo aCGH wash buffers (Agilent Technologies) according
182 to the manufacturer's instructions. Microarrays were scanned using an Agilent high
183 resolution C scanner at a 5 µm resolution with the extended dynamic range setting at 100

184 & 10. Microarray images were processed using feature extraction software v9.5.1.1
185 (Agilent Technologies) utilising linear normalization and rank consistent probe dye
186 normalization methods. Data was processed using GeneSpring GX v7.3.1 (Agilent
187 Technologies) to combine data from replicate spots and multiple node/species reporters.
188 Test samples were normalized to adult control samples to give an estimate of relative
189 abundance.

190

191 **Histology and immunohistochemistry.** Segments of proximal, mid- and distal small
192 intestine were removed from P2 and P9 pups without washing; segments of whole colon
193 was removed from P2 animals and colon from P9 pups was divided into proximal and
194 distal portions, again without washing. Tissues were placed in methanol-Carnoy's
195 fixative and maintained at room temperature for at least 3 h. Paraffin-embedded sections
196 were dewaxed and hydrated; mucin was visualized using anti-MUC2C3 antiserum with
197 Alexa 546-conjugated rabbit immunoglobulins (Life Technologies). Immuno-stained
198 sections were mounted in Prolong Anti-fade (Life Technologies). Images were obtained
199 at room temperature using a Nikon Eclipse E1000 fluorescence microscope with a Plan-
200 Fluor 20x/0.50 DIC M or a 10x/0.30 DIC L objective (Nikon). Images were acquired
201 with a Nikon Digital sight DS5M camera and the Nikon Eclipse E1000 control software.
202 Further processing was performed with Adobe Photoshop software. All image
203 adjustments were performed equally for all comparably stained images.

204

205 **Quantitative PCR.** qPCR was used to amplify and quantify DNA from the bacterial
206 components of the GI tract microbiota; a qPCR assay was developed to enumerate *E.*

207 *coli* K1 in the GI tract. The bacterial load was quantified by amplification of 16S rDNA
208 essentially according to Palmer et al (11). Briefly, universal forward primer 8FM (0.9
209 μM) and *Bifidobacterium longum* forward primer 8FB (0.09 μM) were used in
210 conjunction with universal reverse primer Bact515R (0.9 μM). The thermal cycling
211 program comprised 95°C for 3 min, then 40 cycles of 95°C for 20 s, 55°C for 20 s, 60°C
212 for 35 s, 65°C for 15 s and 72°C for 15 s. *E. coli* K1 was quantified, using a method
213 validated in this study (Supplemental data; Appendix 1), by amplification of the K1-
214 specific gene *neuS* (28). Forward primer neuSF3 (0.625 μM) was used in conjunction
215 with reverse primer neuSR3 (0.625 μM). The *E. coli* K1 thermal cycling program
216 comprised 95°C for 3 min, then 40 cycles of 95°C for 20 s and 61°C for 20 s. In both
217 assays, each 20 μl reaction comprised 1 x Brilliant III SYBR Green Ultra-Fast QPCR
218 Mastermix (Agilent), the assay-specific primers, Rox reference dye (30 nM) and 5 μl
219 extracted DNA. Reactions were performed using a Mx3000P instrument (Stratagene) and
220 fluorescence data for SYBR1 and Rox acquired at the annealing step of each cycle.
221 Tenfold serial dilutions of triplicate genomic DNA extractions from known quantities of
222 *E. coli* strains A192PP (for the *E. coli* K1 assay), and CGSC5073 (for assay of total
223 bacteria) were used to generate standard curves for each qPCR reaction plate. The
224 abundance of *neuS* or 16S rDNA was calculated based on these standard curves using
225 Mx3000P v2.0 software (Stratagene) to normalize SYBR1 to Rox fluorescence and to
226 determine cycle threshold values using adaptive baseline and amplification-based
227 threshold algorithm enhancements. qPCR reaction plates were run in duplicate and
228 contained duplicate standard, sample and no-template control reactions.
229

230 **Semi-quantitative RT-PCR.** cDNA was amplified from RNA extracts by one-step RT-
231 PCR and amplicons resolved by agarose gel electrophoresis. RT-PCR reactions were
232 prepared in a C2BSC to reduce the risk of contamination. RNA (50 ng) was mixed with
233 Brilliant II RT-PCR master mix (Agilent), gene-specific forward and reverse primer pairs
234 (0.5 μ M each) and AffinityScript RT/RNase block enzyme mixture (Agilent) to a final
235 reaction volume of 25 μ L. Control reactions without RNA template or RT/RNase block
236 enzyme were also prepared. RT-PCR was performed using a thermocycling program of
237 30 min at 50°C and 10 min at 95°C, followed by 35 cycles of 30s at 95°C, 1 minute at
238 60°C and 30 s at 72°C. Reactions were mixed with 5 μ L of 6 x Gel Loading Buffer
239 (0.05% w/v bromophenol blue, 40% w/v sucrose, 0.1 M pH 8 EDTA, 0.5% w/v SDS) and
240 resolved by agarose gel electrophoresis. Gels were visualized using a Molecular Imager
241 FX system (Bio-Rad) set to detect UV fluorescence.

242

243 **Gene expression analysis.** RNA was extracted from GI tissues using Qiagen RNeasy
244 Animal Tissue Midi Kit (Qiagen). RNA integrity and concentration were determined with
245 a NanoDrop 1000 (Thermo Scientific). Labeled cDNA was hybridised to Affymetrix
246 GeneChip Rat Genome 230 2.0 arrays. The arrays comprised over 31,000 probe sets
247 representing variants from greater than 28,000 rat genes; there are eleven probe sets
248 represented for each coding sequence. GeneChip expression analysis was performed
249 using samples extracted from uninfected rat pups of age comparable to the reference
250 control. Labeled cDNA synthesis, fragmentation, hybridisation, washing and scanning of
251 rat genome arrays were performed according to the Affymetrix GeneChip Expression
252 Analysis Technical Manual (702232; Rev. 2). Hybridizations were incubated for 16 h at

253 45°C. GeneChips were scanned using Affymetrix Gene Array Scanner 3000.
254 Hybridisation data was analysed on GeneChip Operating Software (GCOS v1.4). DAT,
255 CEL and CHP files were removed using the Data Transfer Tool (v1.1.1); CEL files were
256 imported into the third-party data analysis software GeneSpring v7.3 (Agilent
257 Technologies). GC-RMA normalisation was performed on all data generated using a chip
258 from a comparable uninfected rat pup as reference.

259

260 **Competitive ELISA for Tff2.** Goat polyclonal anti-Tff2 primary antibody (sc-23558;
261 Santa Cruz Biotechnology) was biotinylated, diluted 1:1,000 in blocking buffer (1 % w/v
262 casein in Tris-buffered saline), dispensed in 100 µl aliquots and 10 µg of tissue protein
263 extract added. Serial twofold dilutions of a 15 ng/ml PBS solution of recombinant human
264 Tff2 (rhTff2; Sigma Aldrich) were prepared and 100 µl of each dilution added to
265 individual tubes to give a standard range of 1500-23.4 pg rhTff2. Control tubes
266 containing only anti-Tff2 antibody were also prepared. Standard/antibody,
267 sample/antibody and control tubes were incubated with rotation for 6 h at 20°C.
268 Separately, aliquots (0.1 µg in 100 µl bicarbonate/carbonate buffer pH 9.6) of rhTff2
269 were transferred to each well of 96-well Maxisorp Immunoplates (Nunc), incubated with
270 rotation at 20°C for 2 h, buffer aspirated and wells washed twice with 0.05% v/v
271 Tween20 in PBS. Wells were blocked with 350 µl of blocking buffer, incubated for 2 h,
272 buffer aspirated and the wells washed twice.

273 Standard/antibody, sample/antibody and control solutions were applied to individual
274 wells and plates incubated for 16 h at 20°C. Antibody solutions were aspirated and wells
275 washed four times. HRP-streptavidin conjugate (0.5 µg in 100µl PBS; Vector Labs) was

276 applied to each well, the plates incubated for 1 h, supernatants removed and wells washed
277 four times. Plates were developed by addition of 100 μ l of 3,3',5,5'-tetramethylbenzidine
278 liquid substrate and incubated in the dark for 15-30 min. Color development was
279 terminated by the addition of 100 μ l 0.4 M sulfuric acid. OD₄₅₀ was measured using a
280 SPECTROstar Omega plate-reader (BMG Labtech) and Tff2 quantified by comparison to
281 standard curves obtained by plotting the OD₄₅₀ values against the amount of rhTff2
282 incubated with anti-Tff2 IgG. All standard, sample and control wells were run in
283 triplicate on each plate and each plate was duplicated.

284

285 **Serum cytokine assays.** Serum was obtained by centrifugation (1500 x g; 10 min) of
286 blood collected from culled neonatal rats. Levels of IL-1 β and IL-6 were determined by
287 sandwich ELISA assays, utilising, respectively, rabbit or goat polyclonal cytokine-
288 specific capture and biotinylated detection antibodies and recombinant rat cytokine
289 standards from an appropriate ELISA Development Kit (Peprotech). Reactions were
290 developed by incubation with streptavidin-HRP conjugate (Vector Labs) for 30 min
291 followed by incubation with 3,3',5,5'-tetramethylbenzidine. Reactions were terminated
292 after 15 min by addition of 0.5 M H₂SO₄ and A_{450nm} measured using a SPECTROstar
293 plate-reader (BMG Labtech). All assays were performed in triplicate in 96-well
294 MaxiSorp immunoplates (Nunc).

295

296 **Extraction of tissue cell nuclear proteins.** Prior to extraction of nuclear proteins, single
297 cell suspensions were obtained from whole tissue samples. Tissues were washed in 2 ml
298 ice-cold PBS then transferred to 4.7 ml HEPES buffer (10 mM HEPES, 150 mM NaCl, 5

299 mM KCl, 1 mM MgCl₂, 1 mM CaCl₂) supplemented with collagenase (2 mg/ml) and
300 DNase I (80 U/ml). Samples were homogenized for 10 s on ice, incubated at 37°C for 30
301 min and homogenized for 10 s. Homogenates were filtered (100 µm Cell Strainer; BD
302 Falcon) and tissue cells recovered by centrifugation (500 x g; 10 min). Cell pellets were
303 suspended in 5 ml nuclear extraction buffer (0.32 M Sucrose, 10 mM Tris-HCl, 3mM
304 CaCl₂, 2 mM MgOAc, 0.1 mM EDTA, 1 mM DTT) supplemented with 0.5% v/v NP-40
305 to lyse the plasma membrane, followed by centrifugation (500 x g; 5 min) to obtain
306 nuclei. After aspiration of the cytoplasmic protein fraction, nuclei were washed twice in
307 nuclear extraction buffer and recovered by centrifugation (500 x g; 5 min). Nuclei were
308 suspended in 1.5 ml low salt buffer (20 mM HEPES, 1.5 mM MgCl₂, 20 mM KCl, 0.2
309 mM EDTA, 25% v/v glycerol, 0.5 mM DTT) and lysed by the gradual addition of an
310 equal volume of high salt buffer (20 mM HEPES, 1.5 mM MgCl₂, 800 mM KCl, 0.2 mM
311 EDTA, 25% v/v glycerol, 0.5 mM DTT, 1% v/v NP-40). Samples were incubated for 45
312 min at 4°C on a rotator then centrifuged (14000 x g; 15 min). The nuclear protein fraction
313 was aspirated and stored at -80°C prior to analysis. All nuclear protein extraction buffers
314 were supplemented with 1 x Complete Mini EDTA-free protease inhibitor cocktail
315 (Roche).

316

317 **NF-κB electrophoretic mobility shift assay.** A fluorophore-labeled double stranded
318 oligonucleotide probe containing the NF-κB consensus binding site was prepared by
319 annealing equimolar volumes of 5'-Cy5 conjugated sense and antisense single stranded
320 oligonucleotides at room temperature for 10 min. Binding reaction mixtures were
321 prepared from 1 µl poly-dIdC (1 mg/ml), 3 µl 5 x binding buffer (50 mM Tris-HCl, 750

322 mM KCl, 2.5 mM EDTA, 0.5% v/v Triton X-100, 62.5% v/v glycerol, 1 mM DTT), 5 µg
323 nuclear protein extract, 1 µl labeled probe (10 ng/µl) and ddH₂O in a total volume of 15
324 µl. Reaction mixtures were incubated at room temperature for 30 min prior to
325 electrophoresis on 5 % v/v polyacrylamide gels. Cy5 fluorescence was detected using a
326 Molecular Imager FX scanner (Bio-Rad).

327

328 **RESULTS**

329 **Translocation of *E. coli* K1 to the blood compartment and capacity to cause lethal**
330 **infection is dependent on the age of the colonized host.** The septicemia isolate *E. coli*
331 A192 efficiently colonized the GI tract of neonatal rat pups (frequency of 100%) but only
332 23% (17) to 35% (15) of colonized pups progressed to the bacteremic state. We therefore
333 enhanced the capacity of the A192 strain to translocate to the blood compartment by two
334 rounds of serial passage in neonatal rats. Bacteria recovered from the blood following
335 passage produced bacteremia at higher frequency (100% of colonized pups); one colony
336 from blood culture was propagated for further experimentation and designated strain
337 A192PP. Feeding of *E. coli* A192PP to two-day-old (P2) pups resulted in 100%
338 colonization of the GI tract within 24-48 h; 48 h after dosing, *E. coli* K1 began to appear
339 in the bloodstream and by day 7 all animals had succumbed to a lethal bacteremia (Fig.
340 1A). P5 pups were less susceptible to infection, with, typically, around 50% of animals
341 displaying bacteremia following GI tract colonization rates of 100%. P9 animals were
342 efficiently colonized by A192PP but were refractory to bacteremia and lethal infection
343 (Fig. 1A). Patterns of colonization and infection were highly reproducible in Wistar rat
344 pup litters. For practical reasons, fecal material could only be sampled from the perianal

345 area and the colonization lag displayed in Fig. 1A is likely to be due to increasing
346 contamination of this anatomical region (engendering an increasingly large coliform
347 population) over the first week of life. There was an age-dependent decrease in
348 susceptibility to lethal infection over the P2 to P9 period (Fig. 1B); pups began to acquire
349 resistance from day 3 and were completely resistant by day 9. Reductions in
350 susceptibility to infection following colonization will be accompanied by structural,
351 physiological and microbiological changes of GI tract tissues (29, 30) and we therefore
352 undertook parallel histological and immunohistochemical investigations of GI tissue in
353 order to ensure that processes that affect susceptibility to infection can be correlated with
354 the dynamic process of postnatal development of the rat intestine. Over the P2 to P9
355 period, the length of the digestive system (stomach to colon) increased in incremental
356 fashion from a mean of 25.6 cm at P2 to 47.6 cm at P9 and was characterized by rapid
357 postnatal physiological and anatomical development due to expansion of the small
358 intestine and increased differentiation of the cecum (Fig. 1C). As is evident from Alcian
359 blue/PAS stained sections of intestinal tissue from pups over the P2-P9 period (Fig. 2),
360 organ maturation was accompanied by increases in the thickness of the submucosal layer
361 and the number of mucin-containing cells. In accord with others (31), we found no
362 histological evidence for any lack of structural integrity during the early phases of
363 neonatal development. No discernable histological changes occurred 24 h and 48 h after
364 colonization of P2 and P9 pups with A192PP.

365

366 **Systemic infection is unrelated to either the size of the colonizing *E. coli* K1 cohort**
367 **or the composition of the GI tract microbiota.** Translocation of *E. coli* K1 from the

368 neonatal rat GI tract to the blood occurs *via* the mesenteric lymph nodes and each
369 bacterial cell has a low probability of overcoming the mechanical and immunological
370 barriers to gain access to the blood compartment (15), even though neonatal intestinal
371 mucosal barriers may be incompletely developed at birth (32). As selective elimination of
372 the resident GI tract microbiota may facilitate the translocation of bacteria to systemic
373 organs and tissues (33) and as *E. coli* K1 replicates in the neonatal rat intestine
374 concomitant with translocation to the blood (15), we hypothesized that K1 intestinal
375 colonization prior to the acquisition of a fully developed microbiota would permit
376 sufficient replication of the neuropathogen to enable translocation to take place. We
377 therefore determined the qualitative and quantitative bacterial composition of GI tract
378 tissues from P2, P5 and P9 animals using qPCR of conserved 16S small subunit (SSU)
379 rRNA genes and a customized SSU rDNA microarray designed to detect most currently
380 recognized species and taxonomic groups of bacteria; we also quantified *E. coli* K1 from
381 GI tract whole-tissue homogenates using qPCR of the K1-specific *neuS* gene.

382 There was a high degree of similarity, both quantitatively and qualitatively, between
383 the GI tract microbiota of rat litters (Fig. 3; Fig. S1 in Online Supplemental Material); by
384 P2, uninfected pups had acquired large numbers of resident bacteria and the numbers,
385 expressed as CFU/g tissue, did not increase significantly over the P2-P9 period (Fig. 3A).
386 Even at P2, the range of phyla representative of mammalian GI tract bacterial populations
387 (34, 35) was generally present with an abundance comparable to that found in adult feces,
388 although Bacteroidetes comprised a smaller proportion of the GI tract microbiota in P2-
389 P9 rats compared to adult feces (Fig. 3B). The Firmicutes/Actinobacteria and
390 Proteobacteria dominated bacterial populations over the period P2-P9 and there were no

391 significant ($p = >0.57$) differences in the abundance of these phyla in samples from these
392 pups. In accord with observations in human infants (11), Bacteroidetes comprised a
393 smaller proportion of the GI tract microbiota in P2-P9 rats compared to adult feces (Fig.
394 3B) as a result of under-representation of Bacteroides (Fig. S1C). There were no
395 significant differences between P2, P5 and P9 pups with regard to the three dominant
396 phyla (Fig. S1A-C). At species level within these phyla, there were significant differences
397 between pups of the three age groups for only eight species and these are described in
398 Fig. S1D. Less abundant phyla included Acidobacteria, Nitrospina and Fusobacteria. It is
399 noteworthy that the Acidobacteria, a recently established (36) phylum of metabolically
400 versatile bacteria associated in the main with diverse environmental habitats that
401 encompass soil, freshwater habitats and metal-contaminated subsurface sediments (37,
402 38) and are occasionally found in gastrointestinal material (39, 40), were present in all GI
403 tract samples we examined. Similarly, the chemolithoautotrophic bacteria of the phylum
404 Nitrospina (Nitrospora) are generally associated with aquatic environments (41) but were
405 encountered in all groups of neonatal rats. Thus, we found a high degree of comparability
406 in the composition of the neonatal rat gut microbiota over the P2-P9 period and also good
407 qualitative and quantitative accord between neonatal and adult GI tract bacterial
408 populations.

409 No significant differences were found in the capacity of *E. coli* A192PP to colonize
410 and persist in the P2, P5 and P9 GI tract for at least five days following oral
411 administration of a bacterial suspension (Fig. 3C). Immediately after feeding the *E. coli*
412 K1 strain to both P2 and P9 animals, a major portion of the inoculum distributed to the
413 lower intestine and cecum/colon over the following 48 h period (Fig. 3D). Within 24 h,

414 the largest *E. coli* K1 population was found in cecum/colon tissue samples. Significantly
415 larger numbers of *E. coli* K1 were detected in the upper GI tissues of P2-inoculated
416 compared to P9-inoculated neonates at all time points sampled but numbers were
417 comparable in cecum/colon tissues (Fig. 3D). There was clear evidence of extensive *E.*
418 *coli* K1 replication in the GI tract after introduction of strain A192PP (Fig. S2).

419

420 **GI tissue responses to *E. coli* A192PP colonization are notably different in P2 and**
421 **P9 rat pups.** In the first hours and days following birth, there is a distinct expression
422 pattern of innate immune molecules by mucosal epithelia aimed at preventing infection
423 whilst avoiding excessive inflammatory responses to bacteria and their products (6).
424 During early postnatal development, this bias against T_H1-cell-polarizing cytokine-
425 mediated effects alters following exposure to microbes, diminishing T_H2-cell polarization
426 and enhancing T_H1-cell polarization, and these effects are likely to be pronounced in gut
427 tissue due to the rapid accumulation of a complex microbiota. We therefore examined the
428 response of P2 pups to colonization by *E. coli* K1 to determine if any differences in
429 response compared to P9 animals could shed light on the basis of the age dependency of
430 systemic infection. P2 and P9 pups were fed strain A192PP, GI tract tissues were
431 removed after 12 h and duodenum to colon samples prepared for microarray analysis.
432 Arrays were performed by pooling equimolar amounts of RNA extracted from three
433 infected rat pups. Responses were standardized against tissues removed at the same time
434 from non-colonized animals of identical age and processed in identical fashion.

435 Major differences were found in the response of P2 and P9 pups to colonization (Fig.
436 4; Tables S1-S5); A total of 241 genes were up-regulated twofold or more in the P2 GI

437 tract compared to 354 in P9 animals but only 22 genes were common to both data sets.
438 More genes (240) were down-regulated at least twofold in P9 compared to 36 in P2
439 samples, with eight genes common to both (Fig. 4A; Table S6). With both pooled P2 and
440 P9 tissue arrays, up- and down-regulated genes belonged to a wide range of functional
441 categories, with genes involved in growth, differentiation and development, cell
442 metabolism and transcriptional regulation strongly represented (Table S1). In both P2 and
443 P9 tissues, genes encoding MHC Class I and Class II proteins were differentially
444 expressed. For example, *RT1-Aw2*, encoding RT1 class Ib, was the most strongly up-
445 regulated (17.7-fold) gene in P2-colonized GI tissues (Table S2) and *RT1-A3* and *RT1-*
446 *Db1*, encoding RT1 Class I and Class II proteins respectively, were highly down-regulated
447 in P2-colonized tissues (Table S3). In pups colonized at P9, the most prominently up-
448 regulated (11.8-fold) gene was the MHC class II protein-encoding *RT1-Bb* gene and
449 expression of *RT1-Aw2* was also significantly increased (Table S4); *RT1-A3* and *RT1-*
450 *Db1* were also down-regulated in P9 pups (Table S5). These and other MHC genes
451 feature in the relatively short list of genes whose regulation was modulated by
452 colonization in both P2 and P9 tissues, along with genes involved in mRNA splicing,
453 DNA damage repair and protein modification (Table S6). A number of genes involved in
454 initiation of apoptosis, such as *pcdc4*, *stk17b*, *casp2* and *casp3*, were up-regulated in P9-
455 but not P2-colonized tissues (Table S4) and genes encoding anti-apoptotic factors such as
456 *Tgfb2* and *Hspa5* concomitantly down-regulated (Table S5) in P9 only. Also noteworthy
457 was the 2.5-fold up-regulation in P9 but not P2 of *DDX3X*, encoding a helicase that
458 together with *TBK1* is central to the induction of type-1 interferons in response to
459 pathogens (42).

460 A very limited number of genes whose products are likely to be directly linked to the
461 susceptibility of P2 pups to post-colonization infection were differently regulated by
462 colonizing *E. coli* K1 in P2 compared to P9 pups. The genes encoding the α -defensins
463 Defa24 and Defa-rs1 were up-regulated 3.1- and 5.4-fold respectively in colonized P9,
464 but not P2 pups (Table S4). This class of bactericidal peptides, produced by Paneth cells
465 in the small intestine (43, 44), regulates the composition of the intestinal bacterial
466 microbiome (45), control intestinal barrier penetration by commensular and pathogenic
467 bacteria (46) and are necessary for antibacterial defense in the neonate (47). The failure
468 of P2 animals to respond to *E. coli* K1 colonization in similar fashion to P9 pups may
469 enhance the capacity of this neuropathogen to reach the small intestinal epithelium, as α -
470 defensins are thought to limit the bacterial load at the epithelial surface (48). We
471 therefore investigated temporal aspects of α -defensin gene expression in relation to
472 colonization by *E. coli* A192PP. The most highly down-regulated gene (26.4-fold) in P2
473 animals was *tff2*, encoding trefoil factor 2. This small peptide plays a role in GI mucosal
474 protection, stabilizes the mucus layer and enhances intestinal epithelial repair (49). As the
475 mucus layer continues to develop *post partum* in the rat (50) and the goblet cell
476 complement of the P2 gut appears to be low in comparison to P9 and adult animals (Fig.
477 2), we investigated the impact of *tff2* down-regulation on the development of the mucus
478 layer between P2 and P9.

479 Microarray data were validated by qRT-PCR analysis of eleven differentially
480 regulated genes from the P2 (*RT1-Aw2*, *Btg2*, *Cald1*, *Tff2* and *Ins2*) and P9 (*Defa-rs1*,
481 *Pdcd4*, *Clic4*, *Cav*, *Afp* and *Amy2*) datasets. A highly significant ($p < 0.0001$) Pearson
482 correlation was obtained when microarray and qRT-PCR data were compared.

483

484 **GI tract colonization by *E. coli* A192PP modulates *defa24* and *defa-rs1* expression**
485 **over the P2-P9 period of neonatal development.** No information is available regarding
486 temporal aspects of α -defensin gene expression in the rat over the neonatal period. In
487 order to provide context for the modulation of *defa-rs1* and *defa24* by colonizing *E. coli*
488 K1, we determined the expression of these genes in duodenum to colon GI tract tissues
489 from non-colonized pups over the P1-P11 *post partum* period. The level of expression of
490 both genes progressively increased over this period, peaking at P10; over the eleven days,
491 *defa-rs1* expression increased approximately twelvefold and *defa24* fourfold (Fig. 4G).
492 To determine the effects of colonization on these background levels of gene expression,
493 P2 and P9 pups were fed *E. coli* A192PP and gene expression compared to same-age
494 non-colonized animals 6, 12, 24 and 48 h post-colonization by semi-quantitative PCR
495 (Fig. 4B). The data suggested that, in P2 animals, the expression of both genes increased
496 24-48 h after *E. coli* K1 dosing; in P9 pups, increases in *defa24* expression peaked 24h
497 after dosing whereas *defa-rs1* expression continued to increase over the 48 h period in
498 comparison to animals fed broth rather than bacteria. As the levels of *defa24* and *defa-rs1*
499 continue to rise in control pups over this period, providing a changing background upon
500 which to assess the degree of gene modulation resulting from colonization, we quantified
501 levels of gene expression for both genes by qPCR and normalized the data against the
502 normal developmental levels (Fig. 4G).

503 Expression of *defa24* in P2 gut tissues was similar to background levels following *E.*
504 *coli* K1 colonization. In contrast, *defa24* expression in the P9 gut was significantly
505 increased up to 12 h post-colonization but returned to levels comparable to those found in

506 the control group within 24-48 h (Fig. 4D). Levels of *defa-rs1* expression in colonized P2
507 pups remained comparable to those found in control animals over the 48 h period
508 whereas expression was increased at all time points in colonized P9 pups; differences in
509 *defa-rs1* expression between P2 and P9 animals was significant at all time points over
510 this period (Fig. 4E). We conclude that P2 pups, in contrast to P9 rats, are unable to
511 respond to *E. coli* A192PP colonization by up-regulation of expression of α -defensin
512 peptide genes.

513

514 **Suppression of Tff2 in the P2 GI tract by *E. coli* K1 colonization.** We established that
515 *tff2* expression in non-*E. coli* K1-colonized pups increased incrementally from P1 up to
516 P9 but substantially declined over P9-P11 (Fig. 4G). Semi-quantitative PCR indicated
517 that *tff2* expression was down-regulated over the 48 h post-colonization period in P2 but
518 not P9 pups (Fig. 4B); qPCR confirmed that, whereas GI tissue levels of *tff2* in P9-
519 colonized pups did not differ significantly over this period from the normal
520 developmental levels shown in Fig. 4G, *tff2* levels were markedly reduced by
521 colonization at P2 (Fig. 4C). Suppression of gene expression in P2 tissues was evident at
522 24-48 h; the degree of down-regulation compared to expression in P9 pups was highly
523 significant and was tightly correlated with the reduced levels of Tff2 protein found in P2
524 and P9 tissue homogenates (Fig. 4F).

525 Transcription of *tff* genes is repressed by IL-1 β and IL-6 (51); cell stimulation by
526 these pro-inflammatory cytokines leads to release of NF- κ B and C/EBP β from resting
527 state complexes in the cytoplasm and their translocation to the nucleus (52), where they
528 inhibit transcription of trefoil factor genes. We therefore assessed the systemic levels of

529 these cytokines by cytokine-specific ELISA of serum samples obtained from P2 and P9
530 neonates colonized with *E. coli* K1 and compared these to non-colonized animals. A two-
531 to threefold elevation in systemic IL-1 β from levels found in non-colonized controls was
532 observed 6-24 h after feeding *E. coli* K1 in P2-colonized but not in P9-colonized neonates
533 (Fig. S2A). No IL-6 was detected in either colonized or non-colonized P2 neonates;
534 although IL-6 was detected in both colonized and non-colonized P9 cohorts, no
535 significant differences were observed between the experimental groups (Fig. S2B). In
536 order to provide evidence for the role of NF- κ B in *tff2* transcriptional repression, we
537 assessed the extent of NF- κ B localization to intestinal cell nuclei by electrophoretic
538 mobility shift assay using a Cy5-labelled dsDNA probe containing the NF- κ B consensus
539 binding motif incubated with nuclear protein extracts obtained from intestinal tissues of
540 neonates colonized with *E. coli* K1 and broth-fed, non-colonized animals (Fig. S2C).
541 Although a degree of band-shift was observed in all samples, the intensity of the shifted
542 band was greater in colonized, compared to non-colonized, P2 animals. A control assay
543 utilizing non-labeled wild-type and mutant dsDNA competitors yielded reduced band-
544 shift in the wild-type but not the mutant competition reactions, indicating that the band-
545 shift was specific for the NF- κ B binding motif sequence. These results suggest that *E.*
546 *coli* K1 intestinal colonization provokes a significant increase in the release of IL-1 β in
547 P2-colonized pups, leading to increased nuclear localization of NF- κ B.

548 The observation that P2 pups possess fewer goblet cells than P9 rats (Fig. 2) is
549 reflected in less small intestine-associated mucin and a thinner Muc2-immunostaining
550 layer in the colon compared to the infection-resistant P9 neonates (Fig. 5). Less mucin
551 was evident 48 h after oral feeding of *E. coli* K1 (Fig. 5C) compared to broth-fed pups

552 (Fig. 5B), although much of this can be accounted for by a large decrease in Muc2 stored
553 in colonic goblet cells, presumably expelled into the gut lumen in response to *E. coli* K1
554 colonization. At P4, animals are relatively susceptible to *E. coli* K1 infection (Fig. 1B), so
555 the colonic mucin content of animals sham-fed at P2 and culled at P4 (Fig. 5B) may not
556 be sufficient to afford protection against systemic infection.

557

558 **DISCUSSION**

559 The data presented here and by other workers (14, 17) provide compelling evidence that
560 the capacity of *E. coli* K1 to translocate from the GI tract to the bloodstream constitutes
561 the basis of susceptibility to systemic infection in the neonatal rat model. It is generally
562 accepted that the gut microbiota confers colonization resistance, prohibiting both
563 potentially harmful (53, 54) and potentially beneficial (55) microbes from establishing a
564 foothold in the GI tract. This protective role is complemented by the capacity of members
565 of the microbiota to modulate the virulence of some opportunistic pathogens (56, 57). We
566 therefore hypothesized that the gut microbiota of susceptible P2 pups was likely to be less
567 well developed than that of resistant P9 rats and would permit colonizing *E. coli* K1 to
568 reach sufficient numbers in the GI tract to allow transit to the blood; colonial expansion
569 would be denied to *E. coli* K1 in the P9 GI tract.

570 In broad terms, this hypothesis is not supported by our data. Although the intestinal
571 microbiota of P2, P5 and P9 pups were quantitatively and qualitatively different from the
572 adult microbiota, they were remarkably similar to each other. Even two days *post partum*
573 a highly complex bacterial consortium had developed in the GI tract that was barely
574 distinguishable from that found in P9 animals. However, the methods used in this

575 investigation do not take into account spatial aspects of the distribution of the microbial
576 population. The individual GI compartments have distinct biochemical and physical
577 properties and represent diverse ecological niches. Accordingly, the gastric, small
578 intestinal and colonic compartments play host to a partially distinct subset of the GI
579 microbiota (58, 59, 60) and it is possible that significant changes to the microbiota of
580 these regions occur over the P2-P9 period in a way that could influence susceptibility to
581 infection.

582 The microbiota appeared to exert little influence on the capacity of *E. coli* A192PP to
583 stably colonize the GI tract of P2-P9 pups, notwithstanding that the strain was selected
584 for this study on the basis of its systemic virulence following GI tract colonization. No
585 differences in the *E. coli* K1 burden after colonization at P2, P5 or P9 could be
586 demonstrated after 120 h and the temporal development of the K1 population was very
587 similar in these age groups. We did, however, note some significant differences in the
588 temporal and spatial distribution of *E. coli* A192PP along the GI tract that almost
589 certainly relate to differences in innate competence between P2 and P9 pups, lending
590 support to the contention that the bacteria are more likely to translocate from the small
591 intestine than the colon. The stabilization of the *E. coli* K1 intestinal load 24 h after
592 colonization indicates that there may be an upper limit to the size or growth capacity of
593 the bacterium in the neonatal intestine. The population climaxed immediately prior to the
594 bacterial translocation window, suggesting that a critical *E. coli* K1 population density
595 must be reached before translocation to the blood compartment can occur.

596 The intestinal tissues are subject to significant *post partum* development in response
597 to exposure to the extra-uterine environment and the initiation of enteral feeding.

598 Changes include the proliferation of two secretory epithelial cell lineages which play a
599 key role in maintaining intestinal barrier function in the small intestinal and colonic
600 compartments. The colonic goblet cell population continues to expand *post partum* and is
601 accompanied by increased production of Muc2 and trefoil peptides (61, 62). The small
602 intestinal Paneth cell population also proliferates rapidly in the postnatal period (63), as
603 does their secretion of antimicrobial peptides (64). The proteins secreted by these cells
604 are vital for maintaining the microbiota away from the enteric epithelial surface (65, 66).
605 The fact that they are developmentally regulated indicates that the intestinal barrier
606 function in younger neonates is immature and partly informed our view that the
607 development of the neonatal intestine over the P2-P9 period modulates susceptibility to
608 *E. coli* K1 systemic infection.

609 The neonatal intestinal tract grew substantially over the P2-P9 period and was
610 accompanied by a significant degree of developmental gene regulation. Based on our
611 observations and the current state of knowledge regarding the developmental regulation
612 of Paneth (40) and goblet cells (67), we propose a model to account for the development
613 of innate defense barriers in the neonatal rat intestine over the P2-P9 period (Fig. 6).
614 Thus, at P2 the ileum secretes lower quantities of α -defensins and the colon lower
615 quantities of Muc2 and trefoil factor than at P9, resulting in an underdeveloped stratified
616 inner mucus layer in comparison to P9 pups that permits closer association between the
617 intestinal microbiota (which inhabit the outer mucus layer) and the intestinal epithelium.
618 The comparative lack of α -defensin expression in P2 tissues indicates that the
619 antimicrobial peptide-dependent barrier function of the small intestine is weaker at P2
620 compared to P9 and is likely to be a factor that determines the differences in *E. coli*

621 A192PP numbers along the GI tract. In future work, we will examine the possibility that
622 defects in α -defensin-mediated barrier function allow K1 colonizers to penetrate
623 enterocytes in P2 pups. The development of the colonic mucus barrier may be related to
624 the transient increase in Tff2 expression from P2-P9. Expression of Tff3 in the rat colon
625 does not start to increase towards adult levels until P12-P17 (58, 68); given the apparent
626 role of Tff3 as a structural component of the colonic mucus barrier (69), this pattern of
627 developmental expression seems unusual. Tff2 may play a similar role to Tff3 in the early
628 neonatal intestine, stabilizing the developing colonic mucus barrier prior to the
629 developmental increase in Tff3 expression, or it may be localized to the small intestine
630 rather than the colon.

631 The transcriptional responses of P2 and P9 intestinal tissues to colonization by *E. coli*
632 K1 were highly divergent. Several genes encoding products involved in host defense
633 were differentially expressed, including developmentally regulated α -defensins and Tff2.
634 There were comparatively few differentially expressed genes shared between colonized
635 P2 and P9 neonates, indicating that the intestinal tissue of the refractive neonate responds
636 very differently to that of the susceptible neonate and may in part determine susceptibility
637 to systemic infection. Suppression of Tff2 with concomitant loss of Muc2 in P2-
638 colonized tissues may allow *E. coli* K1 to gain access to the intestinal epithelium.
639 Conversely, the up-regulation of α -defensins by P9-colonized tissues may prevent this
640 interaction. Thus, we propose (Fig. 6) that in P2 animals, the relative deficiency of α -
641 defensins allows the pathogen to access and invade the tissues of the small intestine [1];
642 bacterial colonization is detected by intestinal leucocytes [2]; activated leucocytes secrete
643 IL-1 β , which activates NF- κ B transcription factor [3]; activated NF- κ B suppresses trefoil

644 factor in goblet cells with concomitant breakdown of the inner mucus layer structure [4],
645 allowing bacteria to access and invade colonic tissue [5]. In P9 pups, up-regulation of α -
646 defensins denies the bacteria access to tissues of the small intestine [1] and prevents IL-
647 1β secretion by leucocytes [2]; a thick and intact inner mucus layer prevents bacterial
648 access to colonic tissue [3]. In all likelihood, the mucus layer keeps the colonizing
649 bacteria away from the gut wall, preventing interactions with the epithelial surface.
650 Evidence that *E. coli* K1 cells gain access to the enterocytes in susceptible pups will
651 provide strong support for this model and such interactions will be sought using
652 immunohistochemical procedures. The model would be further strengthened by
653 demonstration that *E. coli* K1 colonization of α -defensin knockout rats at P9 induces the
654 bacteremic state and we are actively pursuing this line of investigation.

655 *E. coli* K1 colonization of the P2 intestine invariably results in translocation of the
656 pathogen from the intestine into the systemic circulation. The site or sites of translocation
657 have yet to be resolved and the proximal small intestine is a likely candidate. However,
658 developmental deficits appear to be present in the P2 small intestinal and colonic barriers
659 and consequently both regions represent a potential route of invasion. Lack of secreted α -
660 defensins could allow *E. coli* K1 to access the small intestinal epithelium. Alternatively,
661 dysregulation of Tff2 expression may provide access to the colonic epithelium. We have
662 provided some indication that *tff2* transcriptional repression involves IL- 1β and NF- κ B.
663 Colonization of the P2 intestine induces the secretion of IL- 1β into the systemic
664 circulation, but this could be due to the early presence of bacteria in the blood; we
665 therefore plan to examine cytokine levels in tissues in more detail in order to provide a
666 mechanistic basis for susceptibility to infection. This is most likely due to the detection of

667 PAMPs by the intestinal leukocyte population. Adult intestinal macrophages lack the
668 CD14 receptor which systemic macrophages use to detect bacterial lipopolysaccharide
669 (70). Lipopolysaccharide tolerance prevents intestinal macrophages from inducing
670 potentially damaging inflammatory reactions in response to the intestinal microbiota;
671 tolerance does not develop until the perinatal period (71, 72) and may explain why IL-1 β
672 secretion is not induced in P9 neonates. Further, α -defensins represent another potential
673 inhibitor of IL-1 β secretion from macrophages in the P9 intestine (73).

674 *E. coli* K1 colonization at P2 may suppress Muc2 synthesis or induce goblet cells to
675 expel stored Muc2 into the intestinal lumen in an attempt to clear the pathogen from the
676 intestine, an effect that has been observed following colonization by the rodent intestinal
677 pathogen *Citrobacter rodentium* (74, 75). The loss of stored Muc2 at such an early stage
678 in the development of the colonic mucus barrier could compromise developmental
679 processes and provide a possible route of infection for *E. coli* K1.

680

681 **ACKNOWLEDGMENTS**

682 This study was supported by research grant G0400268 from the Medical Research
683 Council, Swedish Research Council grant 7461 and the Knut and Alice Wallenberg
684 Foundation.

685

686 We thank Ozan Gundogdu and Melissa Martin for advice on microarray procedures. The
687 authors have no conflicting financial interests.

688

689

690 **REFERENCES**

- 691 1. **Harvey D, Holt DE, Bedford H.** 1999. Bacterial meningitis in the newborn: a
692 prospective study of mortality and morbidity. *Semin. Perinatol.* **23**:218-225.
- 693 2. **Brouwer MC, Tunkel AR, van de Beek D.** 2010. Epidemiology, diagnosis, and
694 antimicrobial treatment of acute bacterial meningitis. *Clin. Microbiol. Rev.*
695 **23**:467-492.
- 696 3. **Robbins JB, McCracken GH, Gotschlich EC, Ørskov F, Ørskov I, Hanson**
697 **LA.** 1974. *Escherichia coli* K1 polysaccharide associated with neonatal
698 meningitis. *N. Eng. J. Med.* **290**:1216-1220.
- 699 4. **Korhonen TK, Valtonen MV, Parkkinen J, Väisänen-Rhen V, Finne J,**
700 **Ørskov F, Ørskov I, Svenson SB, Mäkelä PH.** 1985. Serotypes, hemolysin
701 production, and receptor recognition of *Escherichia coli* strains associated with
702 neonatal sepsis and meningitis. *Infect. Immun.* **48**:486-491.
- 703 5. **Rutishauser U.** 2008. Polysialic acid in the plasticity of the developing and adult
704 vertebrate nervous system. *Nat. Rev. Neurosci.* **9**:26-35.
- 705 6. **Levy O.** 2007. Innate immunity of the newborn: basic mechanisms and clinical
706 correlates. *Nat. Rev. Immunol.* **7**:379-390.
- 707 7. **de Louvois J.** 1994. Acute bacterial meningitis in the newborn. *J. Antimicrob.*
708 *Chemother.* **34(Suppl. A)**:61-73.
- 709 8. **Sarff LD, McCracken GH, Schiffer MS, Glode MP, Robbins JB Ørskov I,**
710 **Ørskov F.** 1975. Epidemiology of *Escherichia coli* K1 in healthy and diseased
711 newborns. *Lancet* **i**:1099-1104.

- 712 9. **Schiffer MS, Oliveira E, Glode MP, McCracken G., Sarff LM, Robbins JB.**
713 1976. A review: relation between invasiveness and the K1 capsular
714 polysaccharide of *Escherichia coli*. *Pediatr. Res.* **10**:82-87.
- 715 10. **Obata-Yasuoka M, Ba-Thein W, Tsukamoto T, Yoshikawa H, Hayashi H.**
716 2002. Vaginal *Escherichia coli* share common virulence factor profile, serotypes
717 and phylogeny with other extraintestinal *E. coli*. *Microbiology* **148**:2745-2752.
- 718 11. **Palmer C, Bik EM, DiGiulio DB, Relman DA, Brown PO.** 2007. Development
719 of the human infant intestinal microbiota. *PLoS Biol.* **5**:1556-1573.
- 720 12. **Nassif X, Bourdoulous S, Eugène E, Couraud P-E.** 2002. How do extracellular
721 pathogens cross the blood-brain barrier? *Trends Microbiol.* **10**:227-232.
- 722 13. **Tunkel AR, Scheld WM.** 1993. Pathogenesis and pathophysiology of bacterial
723 meningitis. *Clin. Microbiol. Rev.* **6**:118-136.
- 724 14. **Glode MP, Sutton A, Moxon ER, Robbins JB.** 1977. Pathogenesis of neonatal
725 *Escherichia coli* meningitis: induction of bacteremia and meningitis in infant rats
726 fed *E. coli* K1. *Infect. Immun.* **16**:75-80.
- 727 15. **Pluschke G, Mercer A, Kuseček B, Pohl A, Achtman M.** 1983. Induction of
728 bacteremia in newborn rats by *Escherichia coli* K1 is correlated with only certain
729 O (lipopolysaccharide) antigen types. *Infect. Immun.* **39**:599-608.
- 730 16. **Mushtaq N, Redpath MB, Luzio JP, Taylor PW.** 2004. Prevention and cure of
731 systemic *Escherichia coli* K1 infection by modification of the bacterial
732 phenotype. *Antimicrob. Agents Chemother.* **48**:1503-1508.

- 733 17. **Mushtaq N, Redpath MB, Luzio JP, Taylor PW.** 2005. Treatment of
734 experimental *Escherichia coli* infection with recombinant bacteriophage-derived
735 capsule depolymerase. *J. Antimicrob. Chemother.* **56**:160-165.
- 736 18. **Martindale J, Stroud D, Moxon ER, Tang CM.** 2000. Genetic analysis of
737 *Escherichia coli* K1 gastrointestinal colonization. *Molec. Microbiol.* **37**:1293-
738 1305.
- 739 19. **Zelmer A, Bowen M, Jokilammi A, Finne J, Luzio JP, Taylor PW.** 2008.
740 Differential expression of the polysialyl capsule during blood-to-brain transit of
741 neuropathogenic *Escherichia coli* K1. *Microbiology* **154**:2522-2532.
- 742 20. **Zelmer A, Martin MJ, Gundogdu O, Birchenough G, Lever R, Wren BW,**
743 **Luzio JP, Taylor PW.** 2010. Administration of capsule-selective endosialidase E
744 minimizes upregulation of organ gene expression induced by experimental
745 systemic infection with *Escherichia coli* K1. *Microbiology* **156**:2205-2215.
- 746 21. **Pluschke G, Pelkonen S.** 1988. Host factors in the resistance of newborn mice to
747 K1 *Escherichia coli* infection. *Microb. Pathogen.* **4**:93-102.
- 748 22. **Polin RA, Harris MC.** 2001. Neonatal bacterial meningitis. *Semin. Neonatol.*
749 **6**:157-172.
- 750 23. **Jennings HJ, Brisson J-R, Kulakowska M, Michon F.** 1993. Polysialic acid
751 vaccines against meningitis caused by *Neisseria meningitidis* B and *Escherichia*
752 *coli* K1, p 25-38. *In* Roth J, Rutishauser U, Troy FA (ed), Polysialic acid.
753 Birkhäuser Verlag, Basel.
- 754 24. **Lee A, Gordon J, Lee C-J, Dubos R.** 1971. The mouse intestinal microflora with
755 emphasis on the strict anaerobes. *J. Exp. Med.* **133**:339-352.

- 756 25. **Achtman M, Mercer A, Kuseček B, Pohl A, Heuzenroeder M, Aaronson W,**
757 **Sutton A, Silver RP.** 1983. Six widespread bacterial clones among *Escherichia*
758 *coli* K1 isolates. *Infect. Immun.* **39**:315-335.
- 759 26. **Gross RJ, Cheasty T, Rowe B.** 1977. Isolation of bacteriophages specific for the
760 K1 polysaccharide antigen of *Escherichia coli*. *J. Clin. Microbiol.* **6**:548-550.
- 761 27. **Palmer C, Bik EM, Eisen MB, Echberg PB, Sana TR, Wolber PK, Relman**
762 **DA, Brown PO.** 2006. Rapid quantitative profiling of complex microbial
763 populations. *Nucl. Acids Res.* **34**:e5.
- 764 28. **Steenbergen SM, Vimr ER.** 2008. Biosynthesis of the *Escherichia coli* K1 group
765 2 polysialic acid capsule occurs within a protected cytoplasmic compartment.
766 *Molec. Microbiol.* **68**:1252-1267.
- 767 29. **Cummins AG, Jones BJ, Thompson FM.** 2006. Postnatal epithelial growth of
768 the small intestine in the rat occurs by both crypt fission and crypt hyperplasia.
769 *Dig. Dis. Sci.* **51**:718-723.
- 770 30. **Hansson J, Panchaud A, Favre L, Bosco N, Mansourian R, Benyacoub J,**
771 **Blum S, Jensen ON, Kussmann M.** 2011. Time-resolved quantitative proteome
772 analysis of *in vivo* intestinal development. *Mol. Cell Proteom.* **10**:M110.005231.
- 773 31. **Pácha J.** 2000. Development of intestinal transport function in mammals.
774 *Physiol. Rev.* **80**:1633-1667.
- 775 32. **Udall JM, Pang K, Fritze L, Kleinman R, Walker WA.** 1981. Development of
776 gastrointestinal mucosal barrier. I. The effect of age on intestinal permeability to
777 macromolecules. *Pediatr. Res.* **15**:241-244.

- 778 **33. Wells CL, Maddaus MA, Reynolds, Jechorek RP, Simmons RL.** 1987. Role of
779 anaerobic flora in the translocation of aerobic and facultatively anaerobic
780 intestinal bacteria. *Infect. Immun.* **55**:2689-2694.
- 781 **34. Andersson AF, Lindberg M, Jakobsson H, Bäckhed F, Nyrén P, Engstrand**
782 **L.** 2008. Comparative analysis of human gut microbiota by barcoded
783 pyrosequencing. *PLoS One* **3**:e2836.
- 784 **35. Ley RE, Hamady M, Lozupone C, Turnbaugh PJ, Ramey RR, Bircher JS,**
785 **Schlegel ML, Tucker TA, Schrenzel MD, Knight R, Gordon JI.** 2008.
786 Evolution of mammals and their gut microbes. *Science* **320**:1647-1651.
- 787 **36. Ludwig W, Bauer SH, Bauer M, Held I, Kirchhof G, Schulze R, Haber I,**
788 **Spring S, Hartmann A, Schleifer KH.** 1997. Detection and *in situ* identification
789 of representatives of a widely distributed new bacterial phylum. *FEMS Microbiol.*
790 *Lett.* **153**:181-190.
- 791 **37. Quaiser A, Ochsenreiter T, Lanz C, Schuster SC, Treusch AH, Eck J,**
792 **Schleper C.** 2003. Acidobacteria form a coherent but highly diverse group within
793 the bacterial domain: evidence from environmental genomics. *Molec. Microbiol.*
794 **50**:563-575.
- 795 **38. Barns SM, Cain EC, Sommerville L, Kuske CR.** 2007. *Acidobacteria* phylum
796 sequences in uranium-contaminated subsurface sediments greatly expand the
797 known diversity within the phylum. *Appl. Environ. Microbiol.* **73**:3113-3116.
- 798 **39. Ley RE, Lozupone CA, Hamady M, Knight R, Gordon JI.** 2008. Worlds
799 within worlds: evolution of the vertebrate gut microbiota. *Nat. Rev. Microbiol.*
800 **6**:776-788.

- 801 40. **Stearns JC, Lynch MDJ, Senadheera DB, Tenenbaum HC, Goldberg MB,**
802 **Cvitkovitch DG, Croitoru K, Moreno-Hagelsieb G, Neufeld JD.** 2011.
803 Bacterial biogeography of the human digestive tract. *Sci. Rep.*
804 **1**:170:10.1038/srep00170.
- 805 41. **Spieck E, Bock E.** 2005. The lithoautotrophic nitrogen-oxidizing bacteria, p 149-
806 153. *In* Garrity G (ed) *Bergey's manual of systematic bacteriology*. Springer,
807 Berlin.
- 808 42. **Soulat D, Bürckstümmer T, Westermayer S, Goncalves A, Bauch A,**
809 **Stefanovic A, Hantschel O, Bennett KL, Decker T, Superti-Furga G.** 2008.
810 The DEAD-box helicase DDX3X is a critical component of the TANK-binding
811 kinase 1-dependent innate immune response. *EMBO J.* **27**:2135-2146.
- 812 43. **Karlsson J, Pütsep K, Chu H, Kays RJ, Bevins CL, Andersson M.** 2008.
813 Regional variations in Paneth cell antimicrobial peptide expression along the
814 mouse intestinal tract. *BMC Immunol.* **9**:37.
- 815 44. **Bevins CL, Salzman NH.** 2011. Paneth cells, antimicrobial peptides and
816 maintenance of intestinal homeostasis. *Nat. Rev. Microbiol.* **9**:356-368.
- 817 45. **Salzman NH, Hung K, Haribhai D, Chu H, Karlsson-Sjöberg J, Amir E,**
818 **Teggatz P, Barman M, Hayward M, Eastwood D, Stoel M, Zhou Y,**
819 **Sodergren E, Weinstock GM, Bevins CL, Williams CB, Bos NA.** 2010. Enteric
820 defensins are essential regulators of intestinal microbial ecology. *Nat. Immunol.*
821 **11**:76-83.

- 822 46. **Vaishnav S, Behrendt CL, Ismail AS, Eckmann L, Hooper LV.** 2008. Paneth
823 cells directly sense gut commensals and maintain homeostasis at the intestinal
824 host-microbial interface. *Proc. Natl. Acad. Sci. U.S.A.* **105**:20858-20863.
- 825 47. **Sherman MP, Bennett SH, Hwang FFY, Sherman J, Bevins CL.** 2005. Paneth
826 cells and antibacterial host defense in neonatal small intestine. *Infect. Immun.*
827 **73**:6143-6146.
- 828 48. **Johansson MEV, Hansson GC.** 2011. Keeping bacteria at a distance. *Science*
829 **334**:182-183.
- 830 49. **Kjelle S.** 2009. The trefoil factor family – small peptides with multiple
831 functionalities. *Cell Molec. Life Sci.* **66**:1350-1369.
- 832 50. **Shub MD, Pang KY, Swann DA, Walker WA.** 1983. Age-related changes in
833 chemical composition and physical properties of mucus glycoproteins from rat
834 small intestine. *Biochem. J.* **215**:405-411.
- 835 51. **Dossinger V, Kayademir T, Blin N, Gött P.** 2002. Down-regulation of TFF
836 expression in gastrointestinal cell lines by cytokines and nuclear factors. *Cell*
837 *Physiol. Biochem.* **12**:197-206.
- 838 52. **Oecklinghaus A, Hayden MS, Ghosh S.** 2011. Crosstalk in NF- κ B signalling
839 pathways. *Nat. Immunol.* **12**:695-708.
- 840 53. **Van der Waaij D, Burghuis JM, Lekkerkerk JE.** 1972. Colonization resistance
841 of the digestive tract of mice during systemic antibiotic treatment. *J. Hyg.* **70**:605-
842 610.
- 843 54. **Fukuda S, Toh H, Hase K, Oshima K, Nakanishi Y, Yoshimura K, Tobe T,**
844 **Clarke JM, Topping DL, Suzuki T, Taylor TD, Itoh K, Kikuchi J, Morita H,**

- 845 **Hattori M, Ohno H.** 2011. Bifidobacteria can protect from enteropathogenic
846 infection through production of acetate. *Nature* 469:543-547.
- 847 55. **McNulty NP, Yatsunenko T, Hsiao A, Faith JJ, Muegge BD, Goodman AL,**
848 **Henrissat B, Oozeer R, Cools-Portier S, Gobert G, Chervaux C, Knights D,**
849 **Lozupone CA, Knight R, Duncan AE, Bain JR, Muehlbauer MJ, Newgard**
850 **CB, Heath AC, Gordon JI.** 2011. The impact of a consortium of fermented milk
851 strains on the gut microbiome of gnotobiotic mice and monozygotic twins. *Sci.*
852 *Transl. Med.* **3**:106ra106.
- 853 56. **Coconnier MH, Lievin V, Lorrot M, Servin AL.** 2000. Antagonistic activity of
854 *Lactobacillus acidophilus* LB against intracellular *Salmonella enterica* serovar
855 Typhimurium infecting human enterocyte-like Caco-2/TC-7 cells. *Appl. Environ.*
856 *Microbiol.* **66**:1152-1157.
- 857 57. **Altenhoefer A, Oswald S, Sonnenborn U, Enders C, Schulze J, Hacker J,**
858 **Oelschlaeger TA.** 2004. The probiotic *Escherichia coli* strain Nissle 1917
859 interferes with invasion of human intestinal epithelial cells by different
860 enteroinvasive bacterial pathogens. *FEMS Immunol. Med. Microbiol.* 40:223-
861 229.
- 862 58. **Eckburg PB, Bik EM, Bernstein CN, Purdom E, Dethlefsen L, Sargent M,**
863 **Gill SR, Nelson KE, Relman DA.** 2005. Diversity of the human intestinal
864 microbial flora. *Science* **308**:1635-1638.
- 865 59. **Hayashi H, Takahashi R, Nishi T, Sakamoto M, Benno Y.** 2005. Molecular
866 analysis of jejunal, ileal, caecal and recto-sigmoidal human colonic microbiota

867 using 16S rRNA gene libraries and terminal restriction fragment length
868 polymorphism. *J. Med. Microbiol.* **54**:1093-1101.

869 60. **Bik EM, Eckburg PB, Gill SR, Nelson KE, Purdom EA, Francois F, Perez-**
870 **Perez G, Blaser MJ, Relman DA.** 2006. Molecular analysis of the bacterial
871 microbiota in the human stomach. *Proc. Natl. Acad. Sci. U.S.A.* **103**:732-737.

872 61. **Chambers JA, Hollingsworth MA, Trezise AE, Harris A.** 1994.
873 Developmental expression of mucin genes *MUC1* and *MUC2*. *J. Cell Sci.*
874 **107**:413-424.

875 62. **Fança-Berthon P, Michel C, Pagniez A, Rival M, Van Seuningen I, Darmaun**
876 **D, Hoebler C.** 2009. Intrauterine growth restriction alters postnatal colonic
877 barrier maturation in rats. *Pediatr. Res.* **66**:47-52.

878 63. **Bry L, Falk P, Huttner K, Ouellette A, Midtvedt T, Gordon JI.** 1994. Paneth
879 cell differentiation in the developing intestine of normal and transgenic mice.
880 *Proc. Natl. Acad. Sci. U.S.A.* **91**:10335-10339.

881 64. **Mallow EB, Harris A, Salzman N, Russell JP, DeBerardinis RJ, Ruchelli E,**
882 **Bevins CL.** 1996. Human enteric defensins. Gene structure and developmental
883 expression. *J. Biol. Chem.* **271**:4038-4045.

884 65. **Johansson ME, Phillipson M, Petersson J, Velcich A, Holm L, Hansson GC.**
885 2008. The inner of the two Muc2 mucin-dependent mucus layers in colon is
886 devoid of bacteria. *Proc. Natl. Acad. Sci. U.S.A.* **105**:15064-15069.

887 66. **Vaishnava S, Yamamoto M, Severson KM, Ruhn KA, Yu X, Koren O, Ley R,**
888 **Wakeland EK, Hooper LV.** 2011. The antibacterial lectin RegIII γ promotes the
889 spatial segregation of microbiota and host in the intestine. *Science* **334**:255-258.

- 890 67. **Kim YS, Ho SB.** 2010. Intestinal goblet cells and mucins in health and disease:
891 recent insights and progress. *Curr. Gastroenterol. Rep.* **12**:319-330.
- 892 68. **Lin J, Holzman IR, Jiang P, Babyatsky MW.** 1999. Expression of intestinal
893 trefoil factor in developing rat intestine. *Biol. Neonate* **76**:92-97.
- 894 69. **Yu H, He Y, Zhang X, Peng Z, Yang Y, Zhu R, Bai J, Tian Y, Li X, Chen W,**
895 **Fang D, Wang R.** 2011. The rat IgGFcγBP and Muc2 C-terminal domains and
896 TFF3 in two intestinal mucus layers bind together by covalent interaction. *PLoS*
897 *One* **6**:e20334.
- 898 70. **Smythies LE, Sellers M, Clements RH, Mosteller-Barnum M, Meng G,**
899 **Benjamin WH, Orenstein JM, Smith PD.** 2005. Human intestinal macrophages
900 display profound inflammatory anergy despite avid phagocytic and bacteriocidal
901 activity. *J. Clin. Invest.* **115**:66-75.
- 902 71. **Lotz M, Gütle D, Walther S, Ménard S, Bogdan C, Hornef MW.** 2006.
903 Postnatal acquisition of endotoxin tolerance in intestinal epithelial cells. *J. Exp.*
904 *Med.* **203**:973-984.
- 905 72. **Maheshwari A, Kelly DR, Nicola T, Ambalavanan N, Jain SK, Murphy-**
906 **Ullrich J, Athar M, Shimamura M, Bhandari V, Aprahamian C, Dimmitt**
907 **RA, Serra R, Ohls RK.** 2011. TGF-β2 suppresses macrophage cytokine
908 production and mucosal inflammatory responses in the developing intestine.
909 *Gastroenterol.* **140**:242-253.
- 910 73. **Shi, J, Aono S, Lu W, Ouellette AJ, Hu X, Ji Y, Wang L, Lenz S, van Ginkel**
911 **FW, Liles M, Dykstra C, Morrison EE, Elson CO.** 2007. A novel role for

912 defensins in intestinal homeostasis: regulation of IL-1beta secretion. *J. Immunol.*
913 **179**:1245-1253.

914 74. **Lindén SK, Florin TH, McGuckin MA.** 2008. Mucin dynamics in intestinal
915 bacterial infection. *PLoS One* **3**:e3952.

916 75. **Bergstrom KS, Kisson-Singh V, Gibson DL, Ma C, Montero M, Sham HP,**
917 **Ryz N, Huang T, Velcich A, Finlay BB, Chadee K, Vallance BA.** 2010. Muc2
918 protects against lethal infectious colitis by disassociating pathogenic and
919 commensal bacteria from the colonic mucosa. *PLoS Pathog.* **6**:e1000902.

920

921

922

923

924

925

926

927

928

929

930

931

932

933

934

935 **LEGENDS**

936

937 **FIG 1.** Age-dependent susceptibility of the neonatal rat to systemic *E. coli* K1 infection.

938 (A) GI tract colonization, bacteremia and accumulated deaths of neonatal rat pups fed *E.*

939 *coli* A192PP two (P2), five (P5) and nine (P9) days after birth. All pups in a litter

940 received the oral dose on day 0. Colonies expressing the K1 capsule were detected using

941 K1-specific bacteriophage from perianal swab cultures and from blood samples. Data

942 shown are from representative experiments involving single litters of 9-14 pups. (B)

943 Survival of P2-P9 rat pups fed *E. coli* A192PP. Two litters (12 pups per litter) of two- to

944 nine-day-old pups were used for each time point and the animals monitored for a period

945 of one week following oral dosing of bacterial cultures; $n=24$, \pm 1SD. (C) Gross

946 morphological appearance of GI tract tissue (stomach to colon) from P1-P9 rat pups.

947

948 **FIG 2.** Rapid development of GI tract tissue morphology during the early postnatal

949 period. Small intestinal (SI) and colonic tissues from P2 and P9 animals were fixed,

950 sectioned and stained with Alcian blue/PAS. The scale bar is 100 μ m.

951

952 **FIG 3.** Comparable rates of GI tract colonization by *E. coli* A192PP over P2-P9 neonatal

953 period complements rapid development of the GI tract microbiota in neonatal rats. (A)

954 Bacterial load, determined by qPCR of conserved 16S SSU rRNA genes, of GI tract

955 tissues and fecal content from P2, P5 and P9 rat pups. At each time point, four animals

956 from each of three litters were sampled. (B) Relative abundance of bacterial phyla of the

957 GI microbiota by SSU rDNA microarray. Data normalized to adult data as indicated by

958 dashed line at $x=1$. Four litters were employed. Four animals removed from each litter at
959 P2, P5 and P9; bacterial DNA extracted from tissue samples at each time point hybridized
960 with DNA from the appropriate maternal fecal sample. Results from each of four litters
961 were combined. Probes ranked according to average Cy5 and Cy3 fluorescence, with the
962 highest at the top of each figure. (C) Temporal aspects of *E. coli* K1 GI tract colonization
963 of P2, P5 and P9 animals. K1 bacteria were quantified by qPCR of the *neuS* gene. DNA
964 extracted from GI tissues and their contents and a calibration curve constructed to convert
965 data to CFU. Two litters of neonatal rats were employed. Four animals were removed
966 from each litter at each time point, the GI tissue removed and processed and DNA
967 representing each time point pooled. LOD: limit of detection. (D) Colonization of the
968 proximal small intestine, distal small intestine and cecum/colon over the 48 h period
969 following feeding of *E. coli* A192PP to P2 and P9 pups. *E. coli* K1 bacteria were
970 quantified by qPCR with the *neuS* probe. Data normalized to tissue mass following
971 conversion to CFUs. Error bars represent the SEM from $n=4$ animals. Significant
972 differences, as determined by 2-tailed Mann-Whitney test: * $p<0.05$, ** $p<0.01$, ***
973 $p<0.001$.

974

975 **FIG 4.** P2 and P9 host responses to *E. coli* K1 intestinal colonization. (A) P2 and P9
976 intestinal tissues show differential transcriptomic responses to *E. coli* K1 colonization as
977 demonstrated by comparison of microarray analysis of RNA extracted from colonized
978 and non-colonized P2 and P9 tissues 12 h post-inoculation with *E. coli* K1 or broth; $n=4$.
979 (B) Expression of *tff2*, *defa24*, *defa-rs1* and the reference gene *rps23* were analyzed by
980 semi-quantitative RT-PCR followed by resolution of pooled cDNA amplicons on agarose

981 gels, and by quantitative qRT-PCR analysis (C, D and E) of RNA extracted from GI tract
982 tissues from colonized and non-colonized P2 and P9 animals 6, 12, 24 and 48 h post-
983 inoculation with *E. coli* K1 or broth. Data from colonized animals were normalized to
984 data from an equal number of non-colonized (broth-fed) animals. Tff2 protein was
985 quantified by competitive ELISA of protein extractions from colonized and non-
986 colonized animals (F). The normal developmental expression of *tff2*, *defa24*, and *defa-rs1*
987 over the P1-P11 period was examined by normalizing qRT-PCR data from non-colonized
988 animals to data obtained from RNA extracted from non-colonized P1 neonatal intestinal
989 tissues (G). Error bars for all figures represent the SEM of results from either n=12 (C, D
990 and E) or n=6 (F) animals. Statistically significant differences, as determined by 2-tailed
991 t-test, between colonized and non-colonized animals are indicated (* $p<0.05$, ** $p<0.01$,
992 *** $p<0.001$).

993

994 **FIG 5.** *E. coli* K1 colonization of P2 pups results in depletion of Muc2 mucin from
995 colonic epithelial cells. Anti-Muc2 immunostaining of sections of colonic tissues from P2
996 (A-C) and P9 (D-F) neonatal rats. Tissues were obtained at P2 (A) or P9 (D) and at 48 h
997 after feeding neonates a control dose (B, E) or *E. coli* A192PP (C, F). The epithelial
998 surface (green line), lumen (L) and stratified mucus layer (white line) are indicated where
999 appropriate. The scale bar is 100 μm .

1000

1001 **FIG 6.** Proposed model of GI barrier development in rats from P2 (A) to P9 (B).
1002 Colonization of the P2 (C) and P9 (D) GI tract by *E. coli* K1. The numbered steps in C
1003 and D are expanded in the text.

FIG 1

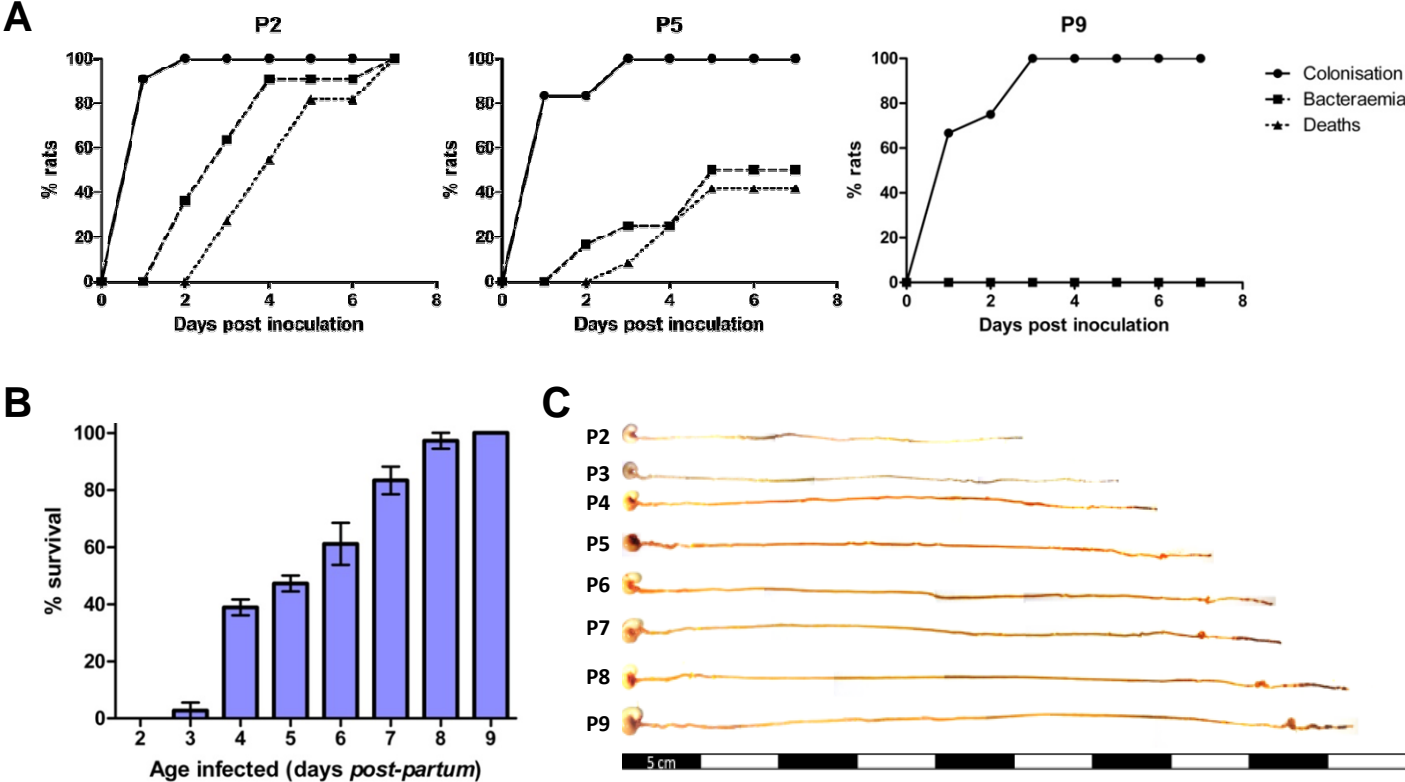


FIG 2

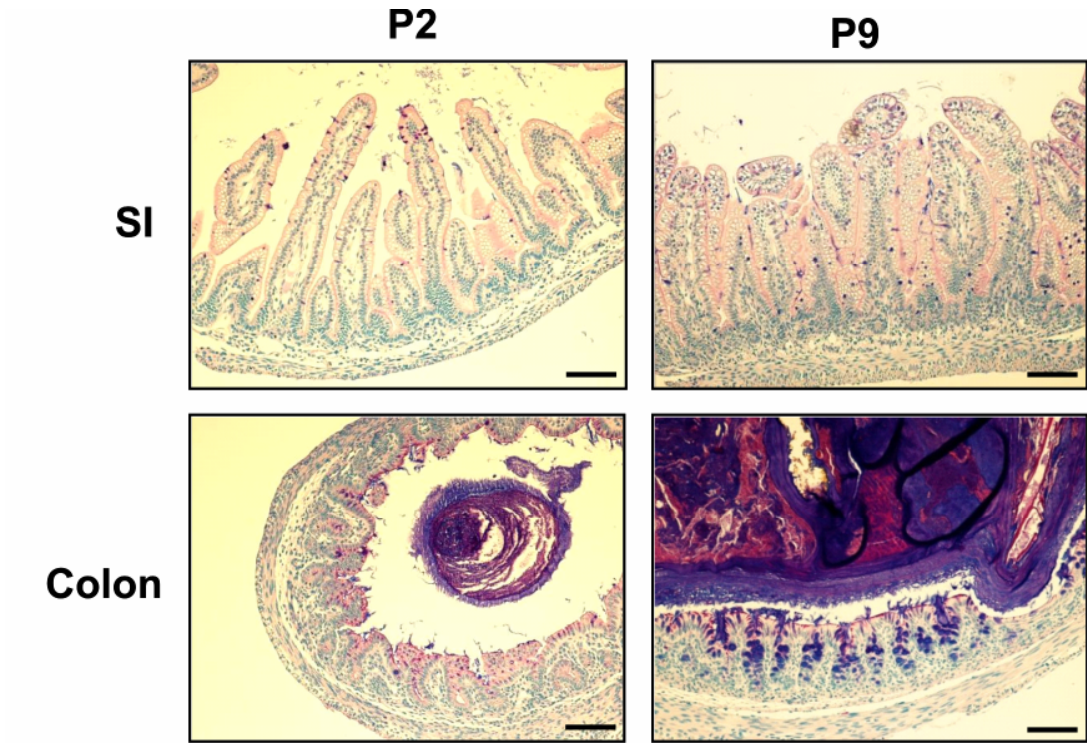


FIG 3

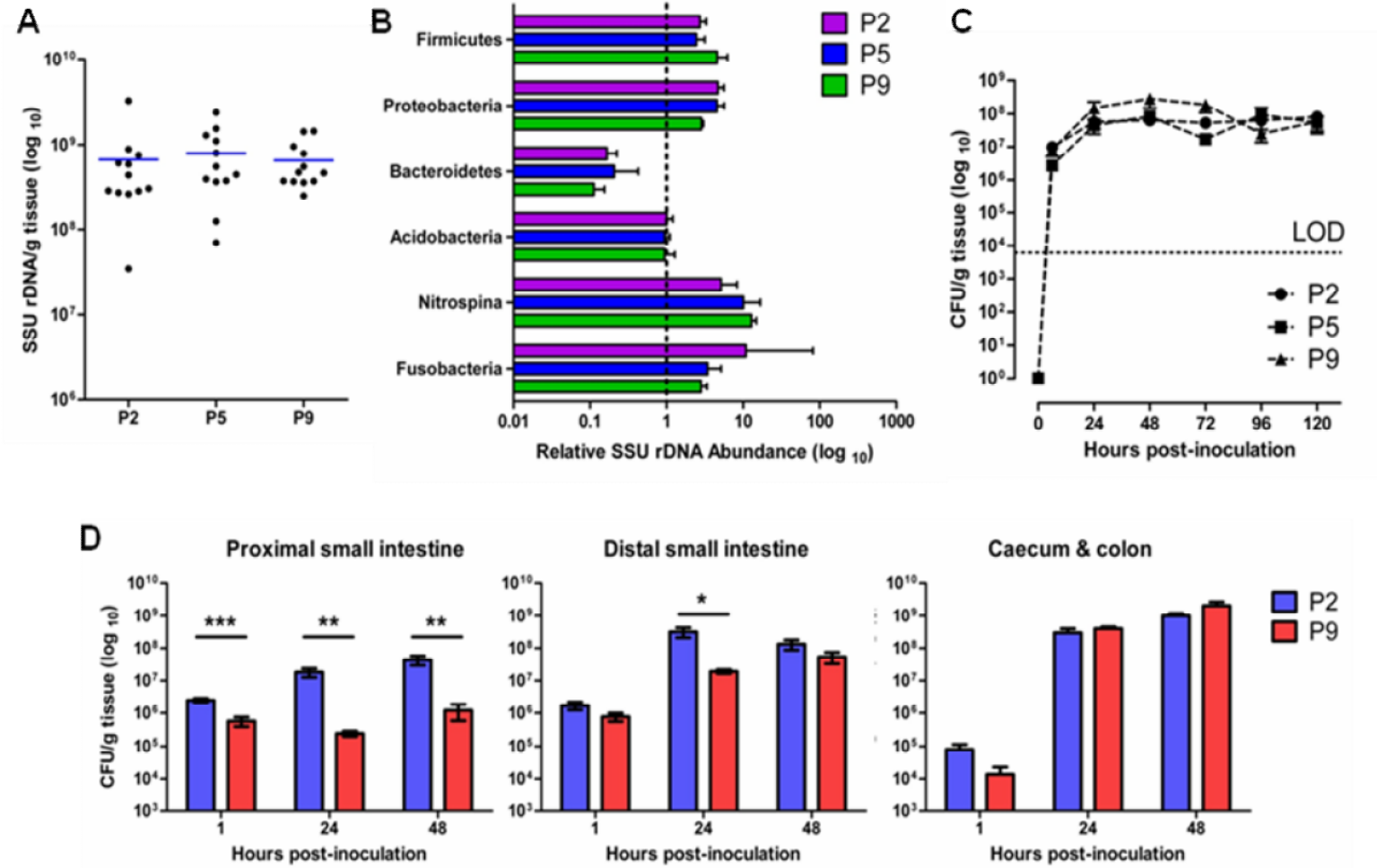


FIG 4

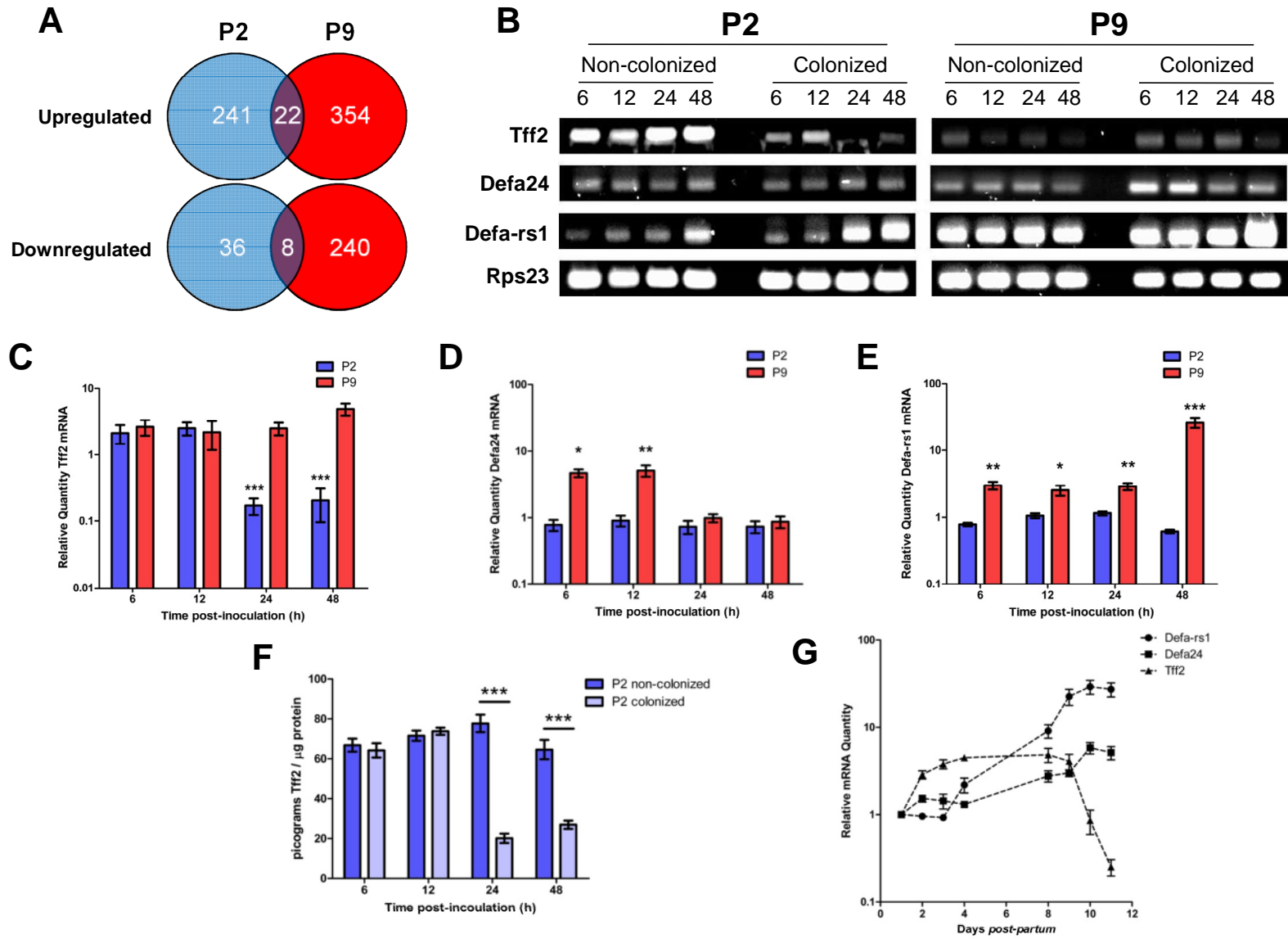


FIG 5

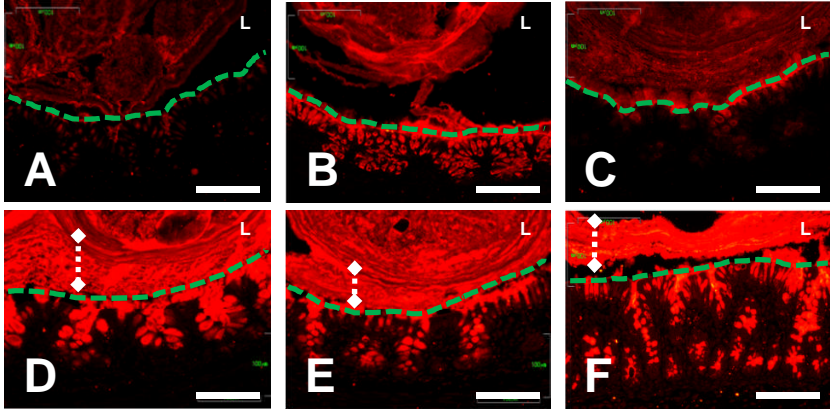


FIG 6

